pH homeostasis during coral calcification in a free ocean CO_2 enrichment (FOCE) experiment, Heron Island reef flat, Great Barrier Reef

Lucy Georgiou[a,b,1], James Falter[a,b], Julie Trotter[a], David I. Kline[c,2], Michael Holcomb[a,b], Sophie G. Dove[c,d,e], Ove Hoegh-Guldberg[c,d,e], and Malcolm McCulloch[a,b]

[a]School of Earth and Environment, The University of Western Australia, Crawley, WA 6009, Australia; [b]Australian Research Council (ARC) Centre of Excellence for Coral Reef Studies, The University of Western Australia, Crawley, WA 6009, Australia; [c]School of Biological Sciences, University of Queensland, St. Lucia, QLD 4072, Australia; [d]ARC Centre of Excellence in Coral Reef Studies, University of Queensland, St. Lucia, QLD 4072, Australia; and [e]Global Change Institute, University of Queensland, St. Lucia, QLD 4072, Australia

Edited by François M. M. Morel, Princeton University, Princeton, NJ, and approved September 1, 2015 (received for review March 20, 2015)

Geochemical analyses ($\delta^{11}B$ and Sr/Ca) are reported for the coral *Porites cylindrica* grown within a free ocean carbon enrichment (FOCE) experiment, conducted on the Heron Island reef flat (Great Barrier Reef) for a 6-mo period from June to early December 2010. The FOCE experiment was designed to simulate the effects of CO_2-driven acidification predicted to occur by the end of this century (scenario RCP4.5) while simultaneously maintaining the exposure of corals to natural variations in their environment under in situ conditions. Analyses of skeletal growth (measured from extension rates and skeletal density) showed no systematic differences between low-pH FOCE treatments (ΔpH = ~−0.05 to −0.25 units below ambient) and present day controls (ΔpH = 0) for calcification rates or the pH of the calcifying fluid (pH_{cf}); the latter was derived from boron isotopic compositions ($\delta^{11}B$) of the coral skeleton. Furthermore, individual nubbins exhibited near constant $\delta^{11}B$ compositions along their primary apical growth axes (±0.02 pH_{cf} units) regardless of the season or treatment. Thus, under the highly dynamic conditions of the Heron Island reef flat, *P. cylindrica* up-regulated the pH of its calcifying fluid (pH_{cf} ~8.4–8.6), with each nubbin having near-constant pH_{cf} values independent of the large natural seasonal fluctuations of the reef flat waters (pH ~7.7 to ~8.3) or the superimposed FOCE treatments. This newly discovered phenomenon of pH homeostasis during calcification indicates that coral living in highly dynamic environments exert strong physiological controls on the carbonate chemistry of their calcifying fluid, implying a high degree of resilience to ocean acidification within the investigated ranges.

ocean acidification | FOCE | Heron Island | coral resilience | pH up-regulation

Atmospheric CO_2 has risen by more than 30% during the last century, causing a reduction in seawater pH of ~0.1 units relative to preindustrial times, with a further reduction of 0.1–0.4 units predicted to occur by the end of this century (1). This process, commonly known as "ocean acidification," is expected to have severe impacts on calcifying marine organisms due to its effect on the thermodynamics of biomineralization (2). Our current understanding of the sensitivity of coral calcification to declining seawater pH has mainly been inferred from short-term laboratory-based studies that do not fully simulate real-world reef conditions, particularly the daily to seasonal variations in temperature, light, and pH (3–5). To address these shortcomings, we applied free ocean carbon enrichment (FOCE) technologies (6–9) to manipulate water chemistry in situ and thereby provide more realistic experimental conditions to investigate how future levels of acidification could affect marine organisms according to different representative concentration pathways (RCPs) (10). The FOCE system uses a flow-through flume design that allows organisms to experience near natural conditions, in particular the daily and seasonal regimes of fluctuating temperature, light, and nutrients while maintaining offsets in flume water pH below that of ambient environmental conditions. This manipulation of the FOCE environment is accomplished by the controlled introduction of small volumes of low-pH modified seawater into the open-ended flumes at levels necessary to simulate future declines in ambient seawater pH. The FOCE system therefore enables realistic simulations of the effects of ocean acidification within natural reef environments at levels of atmospheric pCO_2 that are predicted to occur by the end of this century (10).

The influence that external seawater chemistry (i.e., pH and saturation state) has on biomineralization and ion transport processes during skeleton formation is central to understanding how ocean acidification will affect coral calcification and therefore their general ability to maintain the balance between reef growth and erosion (2). Although a clear understanding of the physicochemical mechanisms controlling coral calcification is still only emerging, an important means of biological control is up-regulation of pH (11, 12) at the site of calcification (pH_{cf}). This pH modification is thought to occur predominantly by the biologically mediated action of Ca-ATPase ion transporters that exchange $2H^+$ for Ca^{2+} (13, 14), but how such biological controls are affected by changes in the ambient marine environment is still poorly understood. It is also becoming increasingly apparent that the natural level of environmental variability to which coral reef systems are subjected to also influences their potential to adapt and/or acclimatize to environmental change (15–17). Understanding how corals living in dynamic environments physiologically respond to large diel and seasonal changes in seawater

Significance

In situ free ocean CO_2 enrichment (FOCE) experiments and geochemical analyses ($\delta^{11}B$, Sr/Ca) conducted on corals (*Porites cylindrica*) from the highly dynamic Heron Island reef flat of the Great Barrier Reef show that this species exerts strong physiological controls on the pH of their calcifying fluid (pH_{cf}). Over an ~6-mo period, from mid-winter to early summer, we show that these corals maintained their pH_{cf} at near constant elevated levels independent of the highly variable temperatures and FOCE-controlled carbonate chemistries to which they were exposed, implying they have a high degree of tolerance to ocean acidification.

Author contributions: L.G. and D.I.K. designed research; L.G. and D.I.K. performed research; L.G., J.F., D.I.K., and M.M. analyzed data; L.G., J.F., J.T., D.I.K., M.H., S.G.D., O.H.-G., and M.M. wrote the paper.

The authors declare no conflict of interest.

This article is a PNAS Direct Submission.

Freely available online through the PNAS open access option.

[1]To whom correspondence should be addressed. Email: lucy.georgiou@research.uwa.edu.au.

[2]Present address: Scripps Institution of Oceanography, Integrative Oceanography Division, University of California at San Diego, La Jolla, CA 92093.

This article contains supporting information online at www.pnas.org/lookup/suppl/doi:10.1073/pnas.1505586112/-/DCSupplemental.

temperature and pH can thus provide important insights into the resilience or vulnerability of corals to ocean warming and acidification. The Heron Island FOCE experiment was thus designed to explore these questions through the application of targeted increases in pCO_2 over an extended time scale to corals living in the highly variable environment of the Heron Island reef flat (9).

The boron isotopic composition ($\delta^{11}B$) of carbonate skeletons essentially records the biologically mediated pH of the calcifying fluid as calcification occurs (11, 12, 18). The use of $\delta^{11}B$ as a pH proxy is based on the selective incorporation of the pH-sensitive and isotopically distinct borate ion, $B(OH)_4$, into the corals' calcium carbonate skeleton (19, 20). Prior studies have shown that the $\delta^{11}B$ of coral skeletons exhibit a significant positive offset from the theoretical borate curve, equivalent to an elevation of ~0.5–0.8 units in the pH_{cf} relative to that of the external seawater pH (11), due to the ability of corals to manipulate their pH_{cf} using energy-dependent ion transporters (13). These observations have been independently corroborated by similar measurements of pH_{cf} using electrodes and pH-sensitive dyes (18, 21, 22). Biological controls on calcification impart significant species-specific but highly systematic increases in pH_{cf} relative to ambient seawater (11). The thermodynamic cost of pH up-regulation within the calcifying fluid, however, is still relatively small compared with the amount of metabolic energy available given normal rates of photosynthesis, respiration, and calcification in reef-building corals (12). Elevation of pH_{cf} above ambient seawater results in higher aragonite saturation states in the calcifying fluid (Ω_{cf}) that in turn drives higher rates of mineral precipitation (12, 21, 23, 24). Understanding the response of pH_{cf} to ocean acidification is therefore critical to predict the effects that increasing levels of atmospheric CO_2 will have on calcification and net reef growth.

Here, we report the sensitivity of pH_{cf} within and between colonies of *Porites cylindrica* grown in situ within a FOCE experiment comprising of flumes subject to both natural (and often extreme) diel and seasonal changes in seawater temperature and pH, as well as enhanced shifts (decreases) in seawater pH to simulate future conditions (10). These experiments were conducted within the highly dynamic reef flat of Heron Island in the Great Barrier Reef (GBR) and covered a range of pCO_2 scenarios (9). We show that *P. cylindrica* corals living in this highly dynamic environment exhibit a previously unrealized strong pH_{cf} homeostasis, despite the highly variable conditions on the reef flat, as well as the superimposed pH offsets (~−0.05 to −0.25 units) in FOCE treatments which simulate future seawater chemistry in a high-pCO_2 atmosphere. We then explore what this apparent lack of sensitivity in pH_{cf} to changes in ambient seawater pH implies for the growth of *P. cylindrica* living in such dynamic environments, as well as how these corals may respond to increasing acidification in a high-pCO_2 world.

Heron Island Reef Flat

Heron Island (23.442°S, 151.914°E) is a subtropical coral cay situated in the southern area of GBR located ~80 km off the coast of Queensland (Fig. S1). The dominant substrate of the inner and midreef flat are carbonate sands that are sporadically populated by coral patches several meters across which typically comprise species of *Acropora* and *Porites*. Tides at Heron Island are semidiurnal, and reef flat waters are separated from the open ocean for a few hours each day at low tide. The shallow depth of the reef flat and periodic isolation at low tide combined with the active metabolism of its benthic communities result in strong diel and seasonal variations in the chemistry of the reef waters (9) (Fig. 1).

Water temperatures offshore of Heron Island range from around 22 °C in winter to around 27 °C during summer. This seasonal temperature pattern is mirrored by the Heron Island reef flat (20 °C to 28 °C, respectively), albeit with slightly larger seasonal amplitudes (6.5 °C vs. 5.5 °C) and stronger diel variations (3–4 °C; Fig. 1*A*). This variability is due to the shallow reef flat waters being more susceptible to local atmospheric heating and cooling,

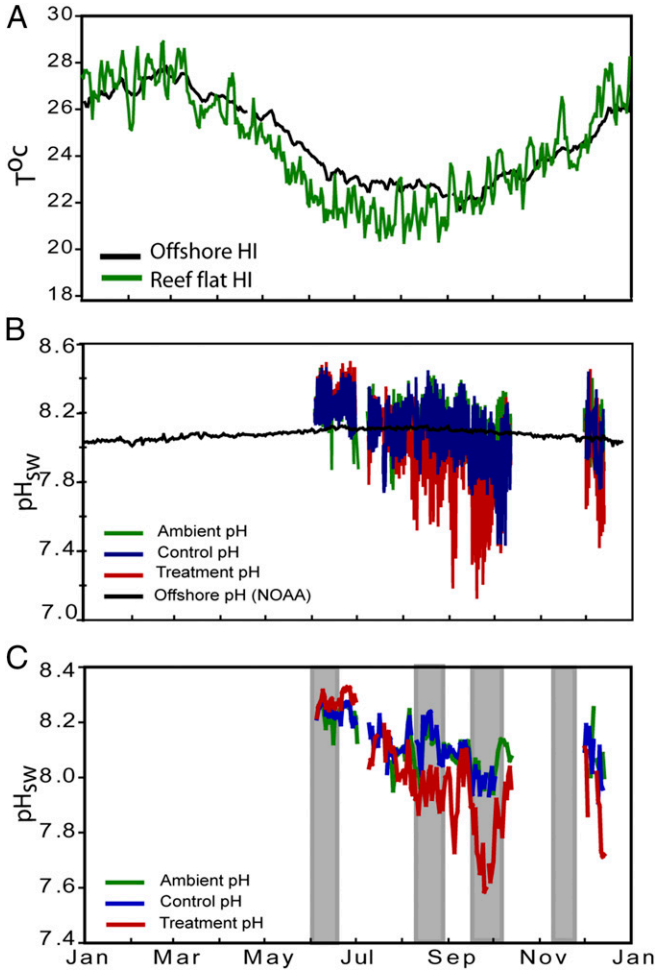

Fig. 1. (*A*) Daily average water temperatures (°C) both offshore (green) and on the Heron Island reef flat (black) from January 2010 to December 2010. (*B*) Daily pH_{sw} (total pH scale) taken at 3-h intervals from end of May 2010 to early December 2010. Offshore data (black), within reef flat data (green), control flume data (blue), and treatment flume data (red). Same color reference applies to *C* except no offshore data shown. gray vertical bars indicate time intervals of milled $\delta^{11}B$ samples. Missing data due to the passing of a tropical storm. Offshore temperature data obtained from a NOAA PMEL CO_2 buoy near Harry's bommie (22.46°S, 151.93°E) managed by the Marine and Atmospheric Research Division of the Commonwealth Scientific and Industrial Research Organization (27) cdiac.ornl.gov/oceans/Moorings/Heron_Island.html. Reef flat temperature data taken from IMOS relay pole #2 (data.aims.gov.au/metadataviewer/uuid/7e3ec622-8f28-4dba-95af-b8075a42241a). Offshore pH data were calculated from records of f_{CO2} data obtained from the Heron Island NOAA buoy assuming an offshore total alkalinity of 2,275 μEq/kg (7). See Fig. S1 for location of loggers and method details. Reproduced from ref. 9.

especially during low tides (9, 25). Similarly seasonal changes in net benthic metabolism (26) result in interseasonal variation in the pH (9) of reef flat waters (~8.24 in June to 8.04 in December) that are much greater than in offshore waters (Fig. 1 *B* and *C*), the latter having relatively constant pH throughout the year (pH ~8.0–8.1) (27). Reef flat waters on Heron Island are also subject to strong diel variations that can change by up to 0.75 pH units within a 24-h period (Fig. S2) (9).

The FOCE system was constructed on the Heron Island reef flat with four submerged flumes (two controls and two treatments) oriented parallel to the shore, each flume open to the environment at both ends and on the bottom. Five living parent colonies of the branching coral *P. cylindrica* were harvested from the Heron Island reef flat and transplanted into both treatment and control

flumes, such that each flume contained a representative selection of each colony. The FOCE flumes were deployed for more than ~6 mo, from the end of May to mid-December 2010.

The FOCE Experiment

Colonies of *P. cylindrica* collected from Heron Island reef flat were first acclimatized for 4 wk before the experiment which commenced in the winter of 2010 (June). In the first phase of the experiment (June to July), all flumes were initially set to follow the same ambient pH conditions of the reef flat waters (mean winter pH ~8.24) to allow colonies to acclimatize further and recover from transplantation. In the second phase of the experiment (July to September), the pH of the FOCE treatment flumes were progressively offset relative to the ambient reef flat water by −0.05 in July, then by −0.15 in August, and finally by −0.25 pH units in September (Fig. 1*C*). The treatment flumes were maintained at this reduced pH offset (−0.25) until early October when the experiment was interrupted by a strong tropical storm that led to a temporary cessation of the pH offset in the FOCE treatments. The experiment then resumed in late November when treatment flumes were again subjected to pH offsets of around −0.25 relative to the ambient seawater pH, which continued until the end of the experiment in mid-December (Table S1). As noted above, both the controls and treatments were subject to strong natural diel and seasonal forcing independent of the FOCE experiment. This strong combined diel and seasonal variation in reef flat pH allowed us to simultaneously examine the response of each coral's internal chemistry to both high levels of natural variability in ambient pH together with systemic shifts in pH expected to occur over this century.

Results and Discussion

The $\delta^{11}B$ compositions (Dataset S1) were measured from a series of subsamples collected along the major growth axis of the skeletons of the *P. cylindrica* nubbins from each of the four FOCE flumes (Fig. S3). High-resolution profiles of strontium to calcium ratios (Sr/Ca; *Materials and Methods*) were used to determine seasonally resolved chronologies and extension rates. Calcification rates along the primary growth axis were calculated from the product of extension rates and density, with the latter determined using the buoyant weight method. Based on the Sr/Ca chronology, the $\delta^{11}B$ compositions were determined for four distinct periods of growth: June, August, late September, and late November 2010 (Fig. 1*C*). The August and especially the late September periods were representative of particularly low pH regimes within the treatment flumes (Fig. 1). Samples analyzed for $\delta^{11}B$ represent ~3 wk of growth and hence incorporate the shorter-term variations in calcification driven by, for example, diel cycles in the supply of metabolic carbon from photosynthesis and respiration (18, 28). During the initial phase of the experiment in midwinter, when the reef flat waters were characterized by relatively high pH (~8.3 units; Fig. 2), the coral nubbins exhibited a wide range of $\delta^{11}B$ values (~22‰ to ~26‰). During the early spring phase (i.e., late September) of the experiment, coral nubbins again exhibited the same range in $\delta^{11}B$ (~22‰ to ~26‰) despite the significant reduction in pH within the FOCE treatments and in the ambient reef flat pH. Importantly, individual nubbins exhibited near constant $\delta^{11}B$ compositions along their major growth axis over each of the four growth periods measured, regardless of whether they were grown under treatment or control conditions (Fig. 2*A* and Fig. S4*A*). These near constant $\delta^{11}B$ compositions equate to near constant internal pH_{cf} (Fig. 2*B* and Fig. S4*B*), irrespective of treatment and season and declined by less than 0.1 units per unit decrease in external pH_{sw} ($\Delta pH_{cf}/\Delta pH_{sw}$= 0.067, P = 0.078, df = 36; Table S2 and Fig. 2*B*). This result reflects the capacity of these coral to homeostatically maintain a pH_{cf} of ~8.4–8.6 at the site of calcification (Fig. 3) and thus near constant up-regulation of pH_{cf} during the calcification process. As such, these findings are in marked contrast to earlier laboratory studies in which corals grown under stable and constant pH conditions

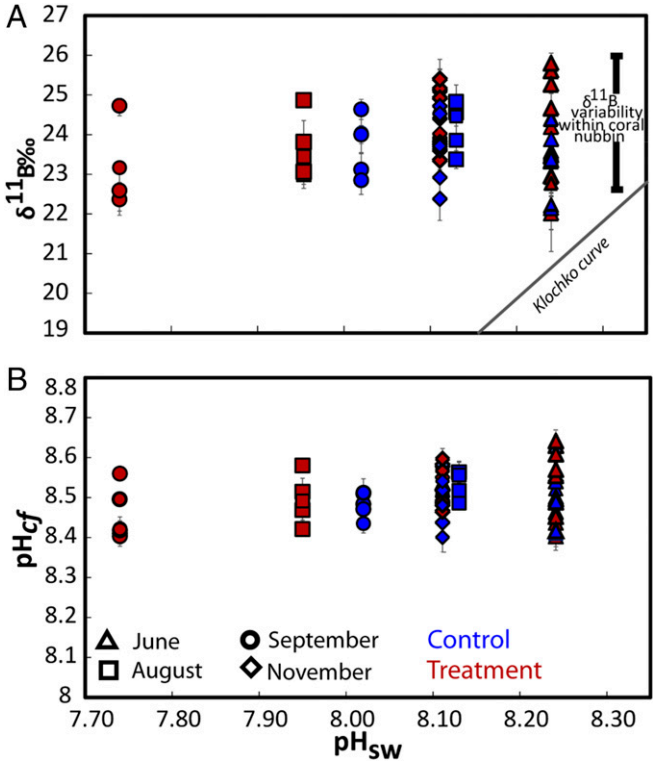

Fig. 2. (*A*) Measured $\delta^{11}B$ composition of all nubbin colonies from treatment (red symbols) and control (blue symbols) flumes vs. the average measured pH seawater conditions at June, August, September, and November 2010 within control and treatment flumes during the FOCE experiment. The boron isotope composition of all samples is elevated relative to the abiotic curve provided by Klochko et al. (50). (*B*) pH of the calcifying fluid (pH_{cf}) derived from the $\delta^{11}B$ shown in *A* using Eq. 2. A linear mixed effects model indicated only a modest dependency of pH_{cf} on pH_{sw} ($\Delta pH_{cf}/\Delta pH_{sw}$= 0.067, P = 0.078, df = 36; Table S2 and Fig. 2*B*).

exhibited a stronger sensitivity to ambient seawater pH, whereby pH_{cf} decreased by up to 0.5 units for each unit decrease in ambient seawater pH. However, under the naturally and highly dynamic pH conditions within the Heron Island reef flat, corals seemingly exert a much stronger physiological control of pH_{cf}, which overrides the seasonal ambient depression in seawater pH, as well as the superimposed FOCE induced decrease in seawater pH. Reinterpretation (11) of previous laboratory work using *P. cylindrica* colonies under depressed pCO_2 conditions (29) indicates that pH up-regulation was taking place at the site of calcification in this species; these previous experiments, however, kept CO_2 constant throughout the experiment and therefore did not capture the dynamic nature of many natural reef environments. We note that the finding from our study of strong pH homeostasis as exhibited along the major growth axis of the coral skeletons occurs despite the large range in $\delta^{11}B$ for intercolonial (Fig. 2) and off-axis intracolony specimens (Fig. S5). The observation of higher $\delta^{11}B$ values for off-axis compared with the primary growth axis of the nubbins (Fig. S5) is unexpected because growth is higher along the primary growth axis, so we can only speculate that factor(s) other than direct pH_{cf} controls on CO_3^{2-}, such as the internal transport of carbon and energy to sites of calcification (30) are driving faster axial growth rates.

Extension rates of *P. cylindrica* nubbins used in both the treatment and control flumes were similar to *P. cylindrica* from elsewhere in the GBR (31); however, this is not entirely surprising given that coral can maintain similar rates of extension under low-pH conditions at the cost of reduced skeletal density and hence rates of calcification (32). Nonetheless, we find that the skeletal densities in

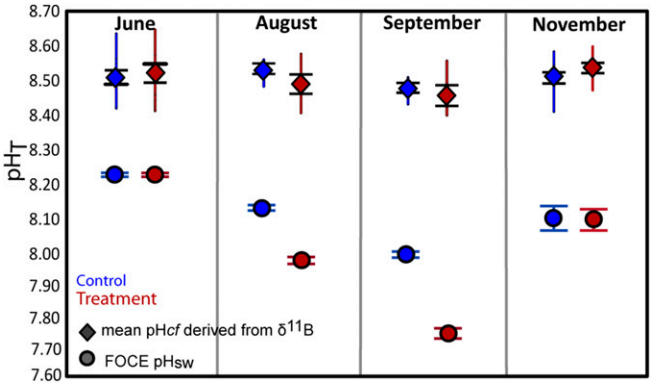

Fig. 3. Boxplots showing range (colored vertical lines) and the mean (diamond) and (±1) SE from the mean (black bars) of pH_{cf} of *P. cylindrica* nubbins taken at four intervals of growth (June, August, September, and November) grown under treatment (red) and control (blue) conditions. Also shown are the mean (circle) and SE (colored horizontal bars) of the pH of the seawater within both treatment (red) and control (blue) FOCE flumes.

the low pH FOCE corals differed by less than 3% from the densities of control corals (Table S3). Furthermore, the calcification rates that we measured were comparable to or higher than rates reported in prior studies (33, 34), which further demonstrates the capacity of *P. cylindrica* from Heron Island reef flat to calcify and grow at normal rates despite the highly variable and disparate thermal and chemical conditions in the controls and in the FOCE treatments.

To better understand how extension and calcification rates varied within and between colonies, we used a "bio-inorganic model" of calcification based on the model of internal pH regulation abiotic calcification (IpHRAC) (12). In this model, the rates of calcification depend primarily on the saturation state of the calcifying fluid (Ω_{cf}) according to known abiotic rate kinetics (24), which are in turn dependent on elevated levels of pH and DIC_{cf} in the calcifying fluid relative to ambient seawater conditions (*Materials and Methods*). We found no significant relationship between rates of extension and estimated saturation state inside the calcifying fluid (Fig. 4*A*), thus providing further evidence that physical rates of coral extension are not strictly dependent on the chemical conditions driving rates of biomineralization within the calcifying fluid. Nonetheless, rates of coral calcification were positively correlated with Ω_{cf} ($r^2 = 0.41$, $P = 0.05$, $n = 10$; Fig. 4*B*), albeit modestly, due to both uncertainties in derived calcification rates (~20%) and the very narrow dynamic range of internal saturation states over which this dependency could be determined ($\Omega_{cf} = 13.5$–16.4 or a relative variation of just 19%). The limited range in Ω_{cf} among experimental colonies was, of course, the direct result of the maintenance of near-constant internal pH_{cf} across treatments and seasons (Fig. 3). Thus, although coral calcification is a biologically mediated process influenced by both external (e.g., light, temperature, food abundance) (35) and internal [e.g., production of organic matrices as templates (36) for skeletal formation] processes, our simple bio-inorganic model nonetheless explains the first-order functional dependence of calcification rates on internal Ω_{cf} (Fig. 4 *A* and *B*).

Our study now provides a process-based mechanism (up-regulation and/or homeostasis of pH_{cf}) that can account for the increased tolerance of corals growing under ranges of ambient seawater pH in highly dynamic reef systems. How sensitive the growth of marine calcifiers is to ocean acidification thus depends on the particular strategies (or lack thereof) for controlling pH at the site of calcification. Based on our findings, we propose three types of strategies: (*i*) the passive strategy whereby pH up-regulation does not occur and rates of calcification follow an abiotic mineral precipitation curve that is highly dependent on ambient pH and pCO_2, and growth in these organisms will be highly sensitive (12) to ocean acidification (e.g., some species of foraminifera); (*ii*) the partial regulation strategy, whereby some up-regulation occurs but the calcifying fluid pH_{cf} is still partially modulated by the external environment (11, 12) and rates of calcification are only partially dependent on ambient pH and pCO_2, and growth in these organisms will be only moderately sensitive to ocean acidification; and (*iii*) the highly resilient or homeostatic strategy, as identified in this study, where a near constant internal (extracellular) pH_{cf} of the calcifying fluid is maintained at a fixed level to optimize calcification rates independent of external conditions, and growth in these organisms will be the least sensitive to ocean acidification. This homeostasis strategy was also observed in the massive corals *Porites lutea* and *P. lobata* during microcosm experiments (37), where the synergetic effects of increased temperature and low pH showed no net effect on calcification rate. The most likely or realistic scenario is that most reef-building corals fall somewhere within the second and third categories; that is, being weaker or stronger partial regulators of internal pH_{cf} depending on their taxonomy, habitat, and/or symbiont composition (11, 12, 22, 38). Indeed, *Porites* appears to be a genus whose adult colonies are highly resilient to ocean acidification, as also shown from their occurrence around CO_2 seeps (39), yet their skeletal densities and calcification rates can nevertheless decline when exposed to particularly caustic seawater chemistries ($\Omega_{sw} < 2$) (40). The variation between and within coral species to maintain robust rates of calcification in low pH (or low Ω_{arg}) conditions may also be a function of their ability to access additional sources of metabolic energy via particle feeding (41).

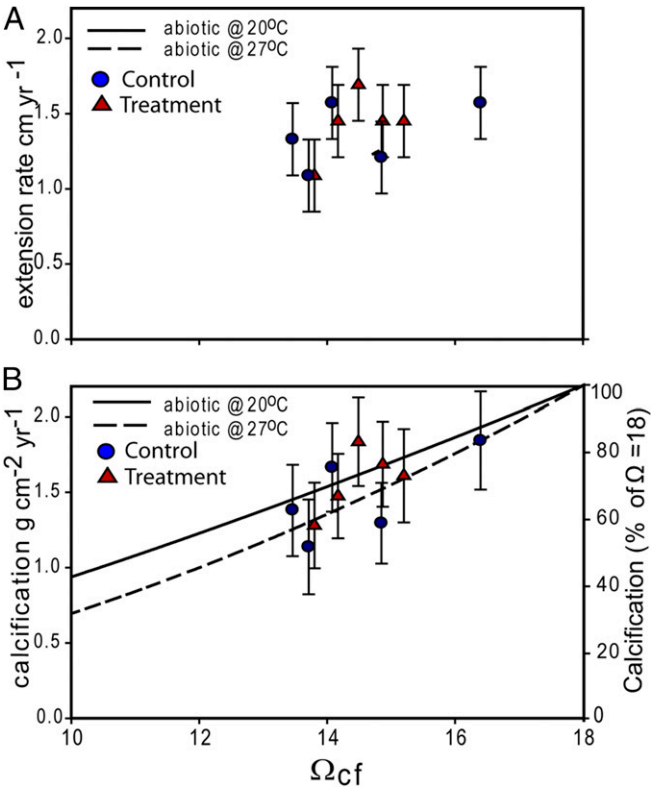

Fig. 4. (*A*) Extension rates of *P. cylindrica* (*y* axis) from both ambient (circles) and elevated pCO_2 (triangles) treatments vs. aragonite saturation state of the calcifying fluid (Ω_{cf}) calculated from boron isotope measurements according to the IpHRAC model of McCulloch et al. (11) (*Materials and Methods*; $r^2 = 0.21$, $P = 0.19$, $n = 10$). (*B*) Calcification rates (left *y* axis) of ambient (circle) and treatment (triangle) *P. cylindrica* corals vs. Ω_{cf} ($r^2 = 0.41$, $P = 0.05$, $n = 10$). Also shown are predicted rates of aragonite precipitation (right *y* axis) as a function of Ω_{cf} relative to $\Omega_{cf} = 18$ at both 20 °C and 27 °C according to the reported abiotic rate kinetics of aragonite precipitation (24).

Nonetheless, naturally occurring acidified reefs ($\Omega_{sw} < 3$) can still support reasonable levels of coral diversity and growth (42), despite any taxa-dependent differences in pH sensitivity.

The capacity of corals to adapt to a changing environment is also expected to vary among species depending on their ability to isolate their growth and metabolism from changes in ambient conditions (12, 43, 44). The results presented herein shows that *P. cylindrica* corals from the Heron Island reef flat maintained elevated extracellular pH_{cf} at the levels necessary to support rates of skeletal growth similar to those recorded in other *Porites* species. Although this capacity for pH_{cf} homeostasis appears to be strongest for *P. cylindrica* colonies growing in more extreme and highly dynamic chemical environments, it is still uncertain how well these coral can maintain this level of pH_{cf} homeostasis with the additional stress of increased temperature (5). To better understand how future reefs may change under high-pCO_2 environments, it is further necessary to assess this potential biological resistance in a range of coral species from environments with different chemical and thermal regimes (5), as well as assess the metabolic cost associated with persistently high pH up-regulation when ambient pH is very low. Regardless, the ability of pH-homeostatic coral to survive and grow in these extreme pH environments may provide them with a greater resilience to the increased levels of ocean acidification expected to occur over the coming decades and centuries.

Materials and Methods

CP-FOCE System. In May 2010, five colonies of *P. cylindrica* were collected from the Heron Island reef flat and divided into subsamples that were allowed to recover on the reef flat for 4 wk before commencing the experiment. In June 2010, the subsamples from each colony were transplanted to each flume to maximize the diversity of the fragments within the flumes and allowed to acclimatize in situ within all four FOCE chambers for a further 4 wk before lowering pH within the flume systems. The pH levels within treatment flumes were then incrementally lowered relative to ambient reef flat water in July (−0.05 pH units), August (−0.15 pH units), and September (−0.25 pH units). The pH within the treatment flumes were then maintained at a constant offset of −0.25 units relative to the controls until early October, when a passing tropical storm interrupted the CO_2 injections and the acquisition of water quality data. The treatments were reinitiated in late November and ran until the end of the experiment (December 2010).

Discrete water samples were collected daily over the course of the experiment for the analysis of dissolved inorganic carbon (DIC), pH, total alkalinity (A_T), and dissolved oxygen. Continuous measurements of pH were made with MBARI digital pH sensors (Nido Instruments), and conductivity, temperature, and depth were measured with a Seabird SBE-16plusV2 SEACAT (Sea-Bird Electronics). For a full description of the FOCE systems, environmental data monitoring, and instrument models/specifications, see refs. 6, 7, and 9.

Sampling Protocol and Geochemical Methods. Coral nubbins were first bleached and then sliced in half to expose the central growth (extension) axis of the coral. One half was used for the analysis of trace elements (to constrain growth chronology), whereas the other half was used for boron isotope analysis. Samples for trace elements were extracted by milling along the major growth axis at 0.5-mm intervals to a depth of 1 mm (see Fig. S3 for diagram) using a video microscope mounted micromill (New Wave Research MicroMill Sampling System; Western Australia Department of Fisheries). Powdered samples (0.5–1 mg) were processed in the ultra-clean laboratory of the Advanced Geochemical Facility for Indian Ocean Research [AGFIOR, University of Western Australia (UWA)] for dissolution and dilution to 10-ppm Ca solutions. Trace element ratios were determined using the Thermo X-series-2 quadropole-inductively coupled plasma mass spectrometer (Q-ICPMS) housed in the UWA AGFIOR facility. Trace element ratios were corrected against an in-house (Davis Reef, NEP) and interlaboratory (JCp-1) coral standards.

Constraining Growth Chronology with Sr/Ca Analysis. Sr/Ca ratios from each coral nubbins (samples of 0.5–1 mg) were measured to provide high resolution (2–4 wk) sampling of ambient seawater temperatures over a roughly 1-y period that began well before commencement of the experiment (Fig. S3 and Dataset S2). Like many other coral, seasonal changes in the Sr/Ca ratios of *P. cylindrical* nubbins were inversely proportional to average monthly reef flat temperatures (45) (Fig. S6). Low Sr/Ca ratios at the apex below the tissue zone of the nubbin (0–1 mm) coincided with higher spring temperatures compared with high Sr/Ca ratios measured between 5 and 7 mm from the apex that coincided with lower winter temperatures. *P. cylindrica* is reportedly a relatively slow growing species, which is consistent with our trace element data that indicates extension rates of ∼1–1.5 mm/mo. Separate Sr/Ca analyses on 5-mg samples conducted during preliminary work also revealed seasonal timing in reef flat temperature minima and maxima that were consistent with the higher-resolution Sr/Ca sampling (Fig. S6). This trace element analysis confirmed the seasonal timing of our boron isotope samples and our ability to follow the primary growth axis back in time.

Extension and Calcification Rates. Linear extension rates were estimated from the physical distance between two points along the primary growth axis identified as occurring in midwinter and early summer according to the Sr/Ca sea surface temperature proxies. Density was calculated using the buoyant weight technique (46), where corals were weighed dry in air before being vacuum sealed in plastic to minimize the effect of air and then submerged and weighed in distilled water. Calcification rates along the primary growth axis were estimated for individual nubbins from multiplying linear extension rates by skeletal densities.

Boron Isotope-pH Proxy. Carbonate samples for boron isotope analysis were extracted along the primary growth axis (Fig. S3) using a small hand held dental drill (Saeshin Strong 206/103L), fitted with diamond burs, at the UWA AGFIOR facility. Sample sizes of 2.5 mg were drilled at the last growth period, representing November (just under the tissue zone), September, August, and the beginning of the experiment (June) as determined from the higher-resolution Sr/Ca data (0.5- to 1-mg samples), from which the time series of seasonal temperatures were derived (Fig. S6). Samples for $\delta^{11}B$ determinations were dissolved in 0.58 N HNO_3, and the boron was quantitatively separated on ion-exchange columns according to McCulloch et al. (47). Boron isotope analyses were measured using the Thermo Neptune Plus Multi Collector-ICPMS and NU Plasma II MC-ICP-MS (AGFIOR, UWA). Isotope data are reported in the permil notation relative to the NIST SRM 951 boron isotopic standard where

$$\delta^{11}B = \left[\left({}^{11}B/{}^{10}B_{sample}/{}^{11}B/{}^{10}B_{std}\right) - 1\right] \times 1{,}000(‰). \quad [1]$$

The pH of the calcifying fluid were derived from measured skeletal $\delta^{11}B_{carb}$ values according to the following equation (48):

$$pH_{cf} = pK_B - \log\left\{\frac{\left[\delta^{11}B_{sw} - \delta^{11}B_{carb}\right]}{\left[\alpha_{B3-B4} \times \delta^{11}B_{carb} - \delta^{11}B_{sw}\right]} + 1{,}000(\alpha_{B3-B4} - 1)\right\}, \quad [2]$$

where pK_B is the dissociation constant dependent on temperature and salinity, $\delta^{11}B_{sw}$ = 39.61 (49), and α_{B3-B4} is the boron fractionation factor for the pH-dependent equilibrium of $B(OH)_4^-$ and $B(OH)_3$ in seawater equal to 1.0272 (50).

Off-axis sampling (Fig. S5*A*) yielded significant differences in $\delta^{11}B$ compositions of up to 2.65‰ (Fig. S5*B*) or up to 0.17 pH units. These significant fine scale spatial controls on $\delta^{11}B$ compositions (18) are also indicative of strong physiological controls on pH_{cf} at the corallite level. To ensure the repeatability of our results and the absence of such sampling artifacts, the initial 5-mg coral nubbin samples (Fig. S7) were replicated by resampling at a higher spatial resolution using 2.5-mg samples (Fig. 2). $\delta^{11}B$ derived from both the 2.5- and 5-mg samples are in close agreement (Fig. 2 and Fig. S7).

Modeling Ω_{cf} and Coral Calcification. Following the IpHRAC model of McCulloch et al. (12), the pH_{cf} of the calcifying fluid was derived from the $\delta^{11}B$ of the nubbin material (Eq. **2**) with the DIC of the calcifying fluid (DIC_{cf}) assumed to be twice that of the treatment and control seawater DIC as calculated from the treatment and control pH, as well as the ambient seawater TA (9). Ω_{cf} for each individual colony were then calculated from pH_{cf} and DIC_{cf}, as well as ambient temperature and salinity (9) using CO_2SYS (51) and averaged over the entire growth period considered (July to December). Hypothetical rates of abiotic calcification (*G*) were calculated over a domain of Ω_{cf} encompassing the average Ω_{cf} of all colonies (Ω_{cf} = 10–18; Fig. 4*B*) and range of temperatures encompassing the experimental period (T = 20–27 °C) according to $G = k(\Omega_{cf} - 1)^n$, where *k* is the rate law constant, Ω_{cf} is the saturation state within the calcifying fluid, and *n* is the order of the reaction (*k* and *n* being temperature dependent) (12). Because the absolute amount of biomineral surface area during calcification is not known at present (38), relative calcification rates were calculated by dividing all modeled calcification rates by the calcification rate achieved when the internal saturation state Ω_{cf} was equal to 18.

Statistics. We used a linear mixed effects model to examine the general dependency of skeletal $\delta^{11}B$ and internal pH_{cf} in *P. cylindrica* on changes in ambient seawater pH (Fig. 2*B*), where each colony was treated as an individual group. All statistical results were generated using the function nlmefit.m in Matlab v8.3.0 (Table S2).

ACKNOWLEDGMENTS. We acknowledge the work of the scientists and engineers that carried out the FOCE experiment at Heron Island in 2010 and thank Dr. Kai Rankenburg from the University of Western Australia Advanced Geochemical Facility for Indian Ocean Research facility for technical assistance with the trace element and isotope analyses. We appreciate assistance from Jan Richards from the Department of Fisheries (Western Australia) for the use of their micromill. Permits from the Department of Environment and Resource Management (CSCE00874010) and the Great Barrier Reef Marine Park Authority (G09/29996.1) were provided to conduct this research. The CP-FOCE experiments were funded by Australian Research Council (ARC) Linkage Infrastructure Equipment and Facilities Grant LE0989608 (to O.H.-G., D.I.K., S.G.D., and M.M.), ARC Linkage Grant LP0775303 (to O.H.-G.), ARC Centre of Excellence Grant CE0561435 (to O.H.-G. and S.G.D.), a Queensland Government Smart State Premier's fellowship (to O.H.-G.), and a Pacific Blue Foundation grant (to D.I.K.). This project was funded by the ARC Centre of Excellence for Coral Reef Studies (University of Western Australia and University of Queensland). Funding support was also provided to L.G. from an Australian Government International Postgraduate Research Scholarship (IPRS) Australian Postgraduate Award (APA) scholarship. M.M. was supported by a Western Australian Premier's fellowship and an ARC Laureate fellowship. M.H. acknowledges support from an ARC Super Science award.

1. Bopp L, et al. (2013) Multiple stressors of ocean ecosystems in the 21st century: Projections with CMIP5 models. *Biogeosciences* 10(10):6225–6245.
2. Hoegh-Guldberg O (2005) Low coral cover in a high-CO2 world. *J Geophysic Res Oceans* 110(C9):C09S06.
3. Ohde S, van Woesik R (1999) Carbon dioxide flux and metabolic processes of a coral reef, Okinawa. *Bull Mar Sci* 65(2):559–576.
4. Hofmann GE, et al. (2011) High-frequency dynamics of ocean pH: A multi-ecosystem comparison. *PLoS One* 6(12):e28983.
5. Dove SG, et al. (2013) Future reef decalcification under a business-as-usual CO2 emission scenario. *Proc Natl Acad Sci USA* 110(38):15342–15347.
6. Marker M, et al. (2010) The coral proto free ocean carbon enrichment system (CP-FOCE): Engineering and development. (OCEANS 2010 IEEE, Sydney), pp 1–10.
7. Kline DI, et al. (2012) A short-term in situ CO_2 enrichment experiment on Heron Island (GBR). *Sci Rep* 2:413.
8. Gattuso J-P, et al. (2014) Free ocean CO2 enrichment (FOCE) systems: Present status and future developments. *Biogeosciences* 11:4057–4075.
9. Kline DI, et al. (2015) Six month *in situ* high-resolution carbonate chemistry and temperature study on a coral reef flat reveals asynchronous pH and temperature anomalies. *PLoS One* 10(6):e0127648.
10. van Vuuren DP, et al. (2011) The representative concentration pathways: An overview. *Clim Change* 109(1-2):5–31.
11. Trotter J, et al. (2011) Quantifying the pH 'vital effect' in the temperate zooxanthellate coral Cladocora caespitosa: Validation of the boron seawater pH proxy. *Earth Planet Sci Lett* 303(3-4):163–173.
12. McCulloch MT, Falter J, Trotter J, Montagna P (2012) Coral resilience to ocean acidification and global warming through pH up-regulation. *Nat Clim Chang* 2(8):623–627.
13. Al-Horani FA, Al-Moghrabi SM, de Beer D (2003) The mechanism of calcification and its relation to photosynthesis and respiration in the scleractinian coral Galazea fascicularis. *Mar Biol* 142(3):419–426.
14. Cohen AL, McConnaughey TA (2003) Geochemical perspectives on coral mineralization. *Rev Mineral Geochem* 54(1):151–187.
15. Oliver TA, Palumbi SR (2011) Do fluctuating temperature environments elevate coral thermal tolerance? *Coral Reefs* 30(2):429–440.
16. Barshis DJ, et al. (2013) Genomic basis for coral resilience to climate change. *Proc Natl Acad Sci USA* 110(4):1387–1392.
17. Palumbi SR, Barshis DJ, Traylor-Knowles N, Bay RA (2014) Mechanisms of reef coral resistance to future climate change. *Science* 344(6186):895–898.
18. Holcomb M, et al. (2014) Coral calcifying fluid pH dictates response to ocean acidification. *Sci Rep* 4:5207.
19. Vengosh A, Chivas AR, Mcculloch MT (1989) Direct determination of boron and chlorine isotopic compositions in geological-materials by negative thermal-ionization mass-spectrometry. *Chem Geol* 79(4):333–343.
20. Hemming NG, Hanson GN (1992) Boron isotopic composition and concentration in modern marine carbonates. *Geochim Cosmochim Acta* 56(1):537–543.
21. Ries JB (2011) A physicochemical framework for interpreting the biological calcification response to CO2-induced ocean acidification. *Geochim Cosmochim Acta* 75(14): 4053–4064.
22. Venn A, Tambutté E, Holcomb M, Allemand D, Tambutté S (2011) Live tissue imaging shows reef corals elevate pH under their calcifying tissue relative to seawater. *PLoS One* 6(5):e20013.
23. Cohen AL, McCorkle DC, de Putron S, Gaetani GA, Rose KA (2009) Morphological and compositional changes in the skeletons of new coral recruits reared in acidified seawater: Insights into the biomineralization response to ocean acidification. *Geochem Geophys Geosyst* 10(7):Q07005.
24. Burton E, Walter L (1987) Relative precipitation rates of aragonite and Mg calcite from seawater:Temperature or carbonate ion control? *Geology* 15(2):111–114.
25. MacKellar MC, McGowan HA, Phinn SR (2013) An observational heat budget analysis of a coral reef, Heron Reef, Great Barrier Reef, Australia. *J Geophys Res, D, Atmospheres* 118(6):2547–2559.
26. Cyronak T, Santos IR, McMahon A, Eyre BD (2013) Carbon cycling hysteresis in permeable carbonate sands over a diel cycle: Implications for ocean acidification. *J Limnol Oceanogr* 58(1):131–143.
27. Tilbrook B, et al. (2013) *High-Resolution Ocean and Atmosphere pCO2 Time-Series Measurements from Mooring Heron Island 152E_23S* (Carbon Dioxide Information Analysis Center ORNL, US Department of Energy, Oak Ridge, TN).
28. Schneider K, Levy O, Dubinsky Z, Erez J (2009) In situ diel cycles of photosynthesis and calcification in hermatypic corals. *Limnol Oceanogr* 54(6):1995–2002.
29. Hönisch B, et al. (2004) Assessing scleractinian corals as recorders for paleo-pH: Empirical calibration and vital effects. *Geochim Cosmochim Acta* 68(18):3675–3685.
30. Fang LS, Chen YWJ, Chen CS (1989) Why does the white tip of stony coral grow so fast without zooxanthellae? *Mar Biol* 103(3):359–363.
31. Jompa J, McCook LJ (2002) The effects of nutrients and herbivory on competition between a hard coral (Porites cylindrica) and a brown alga (Lobophora variegata). *Limnol Oceanogr* 47(2):527–534.
32. Crook ED, Potts D, Rebolledo-Vieyra M, Hernandez L, Paytan A (2012) Calcifying coral abundance near low-pH springs: Implications for future ocean acidification. *Coral Reefs* 31(1):239–245.
33. Hii Y-S, Ambok Bolong AM, Yang T-T, Liew H-C (2009) Effect of elevated carbon dioxide on two scleractinian corals: Porites cylindrica (Dana, 1846) and Galaxea fascicularis (Linnaeus, 1767). *J Mar Biol* 2009:215196.
34. Suggett DJ, et al. (2013) Light availability determines susceptibility of reef building corals to ocean acidification. *Coral Reefs* 32(2):327–337.
35. Allemand D, Tambutté É, Zoccola D, Tambutté S (2011) *Coral Calcification, Cells to Reefs*: *An Ecosystem in Transition*, eds Dubinsky Z, Stambler N (Springer, The Netherlands), pp 119–150.
36. Mass T, Drake JL, Peters EC, Jiang W, Falkowski PG (2014) Immunolocalization of skeletal matrix proteins in tissue and mineral of the coral Stylophora pistillata. *Proc Natl Acad Sci USA* 111(35):12728–12733.
37. Edmunds PJ, Brown D, Moriarty V (2012) Interactive effects of ocean acidification and temperature on two scleractinian corals from Moorea, French Polynesia. *Glob Change Biol* 18(7):2173–2183.
38. Venn AA, et al. (2013) Impact of seawater acidification on pH at the tissue-skeleton interface and calcification in reef corals. *Proc Natl Acad Sci USA* 110(5):1634–1639.
39. Fabricius KE, et al. (2011) Losers and winners in coral reefs acclimatized to elevated carbon dioxide concentrations. *Nat Clim Chang* 1(3):165–169.
40. Crook ED, Cohen AL, Rebolledo-Vieyra M, Hernandez L, Paytan A (2013) Reduced calcification and lack of acclimatization by coral colonies growing in areas of persistent natural acidification. *Proc Natl Acad Sci USA* 110(27):11044–11049.
41. Grottoli AG, Rodrigues LJ, Palardy JE (2006) Heterotrophic plasticity and resilience in bleached corals. *Nature* 440(7088):1186–1189.
42. Shamberger KEF, et al. (2014) Diverse coral communities in naturally acidified waters of a Western Pacific reef. *Geophys Res Lett* 41(2):499–504.
43. Smith LW, Barshis D, Birkeland C (2007) Phenotypic plasticity for skeletal growth, density and calcification of Porites lobata in response to habitat type. *Coral Reefs* 26(3):559–567.
44. Baker AC, Starger CJ, McClanahan TR, Glynn PW (2004) Coral reefs: Corals' adaptive response to climate change. *Nature* 430(7001):741–741.
45. Smith SV, Buddemeier RW, Redalje RC, Houck JE (1979) Strontium-calcium thermometry in coral skeletons. *Science* 204(4391):404–407.
46. Spencer Davies P (1989) Short-term growth measurements of corals using an accurate buoyant weighing technique. *Mar Biol* 101(3):389–395.
47. McCulloch MT, Holcomb M, Rankenburg K, Trotter JA (2014) Rapid, high-precision measurements of boron isotopic compositions in marine carbonates. *Rapid Commun Mass Spectrom* 28(24):2704–2712.
48. Zeebe RE, Wolf-Gladrow DA (2001) *CO2 in Seawater: Equilibrium* (Kinetics, Isotopes) CO_2 in seawater: Equilibrium (kinetics, isotopes). *Elsevier Oceanography Series*, eds Richard EZ, Dieter WG (Elsevier, Munich), Vol 65, pp 1–84.
49. Foster GL, Pogge von Strandmann PAE, Rae JWB (2010) Boron and magnesium isotopic composition of seawater. *Geochem Geophys Geosyst* 11(8):Q08015.
50. Klochko K, Kaufman AJ, Yao W, Byrne RH, Tossell JA (2006) Experimental measurement of boron isotope fractionation in seawater. *Earth Planet Sci Lett* 248(1-2):276–285.
51. Pierrot DE, Lewis DW, Wallace R (2006) *MS Excel Program Developed for CO_2 System Calculations* (Oak Ridge National Laboratory, US Department of Energy, Oak Ridge, TN).